# STRENGTH AND FAILURE OF ALUMINUM ALLOY AMg6 WITH SHOCK-WAVE LOADING

V. K. Golubev, A. I. Korshunov, S. A. Novikov,
Yu. S. Sobolev, and N. A. Yukina

UDC 539.4

Aluminum alloy AMg6 is one of the most extensively used structural materials in modern technology. This is due to its high physicomechanical and production properties, and as for other aluminum alloys, low density and high corrosion resistance. The problem of optimum design of modern structures necessitates more detailed data for the mechanical properties of structural materials, in particular alloy AMg6, over a wide range of loading conditions characterized mainly by test temperature and deformation rate. A comprehensive study of the mechanical properties of alloy AMg6 under static test conditions over wide ranges of deformation rate of $10^{-6}$-0.3 $sec^{-1}$ and temperatures of 80-850°K was carried out in [1]. Data for alloy mechanical properties in the deformation rate range $5 \cdot 10^{-4}$-20 $sec^{-1}$ and temperatures of 0-500°C were given in [2]. For uniaxial tensile conditions at normal temperature a series of results has also been obtained with higher deformation rates up to $4 \cdot 10^4$ $sec^{-1}$ [3-6]. Separately it is necessary to isolate shock-wave test conditions characterized by high intensity and short-term material loading with unidimensional deformation. Here it is possible to note a number of works for the effect of typical loading time and test temperature on the spalling resistance of alloy AMg6 [7-11]. Particular aspects of spalling failure for the alloy have also been considered in [12, 13].

In the present work a task is set for obtaining new experimental data for the effect of test temperature on the strength and failure of aluminum alloy AMg6 with shock-wave loading. The possibility is considered of determining residual mechanical properties for material damaged by spalling in microspecimens prepared from macrospecimens subjected to shock-wave loading. An attempt is made at first to systematize data for the spalling resistance of aluminum alloy AMg6 taking account of the effect of typical loading time, test temperature, and material technology.

Specimens 10 mm thick and 80 mm in diameter for shock-wave testing were cut from sheet and annealed at 320°C for 1 h. Arrangement of the tests was the same as in [10]. Shock-wave loading of specimens was accomplished with impact of a plate of aluminum alloy AMts 4 mm thick accelerated to the required velocity w by glancing detonation of an explosive charge. Specimen heating to 500°C was carried out with an electrical heater. Estimation of pressure in the loading pulses was done as in [10] by the equation $p = \rho(c_0 + \lambda w/2)w/2$, where $\rho = 2.7$ $g/cm^3$, $c_0 = 5.25$ km/sec, $\lambda = 1.39$. Typical loading time, estimated as the time for circulation of a plastic wave in the aluminum striker, is 1.5 $\mu$sec. The degree and nature of spalling failure for loaded specimens was determined directly by metallographic analysis of longitudinal sections. The results obtained for the effect of temperature on spalling failure for alloy AMg6 are given in Fig. 1. Here (a) also gives some additional results from [10] in which specimens prepared from bar in the as-supplied condition were tested. The degree of spalling damage for specimens is nominally divided into a series of grades: 1) retention of material integrity, i.e., absence of spalling microdamage in a cross section with observation at a magnification of ×1000; 2) weak material microdamage, i.e., presence in the spalling zone of individual isolated microdamage observed under a microscope; 3) intense material microfailure, i.e., presence in the spalling zone of a considerable number of isolated and merging areas of microdamage observed under the microscope; 4) weak macrofailure of a specimen, i.e., existence in the spalling zone of small a microcracks observed visually in an etched section; 5) partial spalling failure, i.e., presence in the cross section of individual areas of main crack formation; 6) total spalling failure, i.e., existence of a main spalling crack passing through the whole specimen cross section. Solid and broken lines are critical

Moscow. Translated from Zhurnal Prikladnoi Mekhaniki i Tekhnicheskoi Fiziki, No. 2, pp. 121-128, March-April, 1988. Original article submitted January 26, 1987.

 0021-8944/88/2902-0274$12.50 

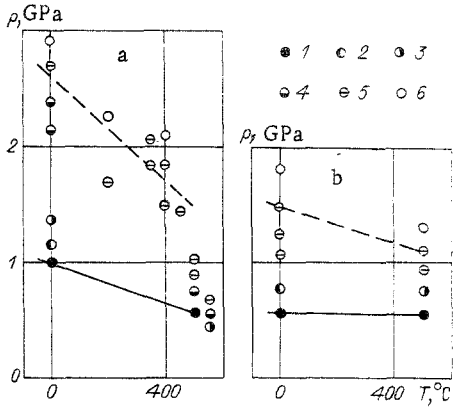


Fig. 1

loading conditions corresponding to microscopic and macroscopic spalling failure of bar (a) and sheet (b) alloy AMg6.

At our suggestion the authors of [11] carried out a test for one of the specimens using the loading and recording methods described there. Specimen shock-wave loading was accomplished by impact of an aluminum foil 0.4 mm thick accelerated by means of an explosive loading device to a velocity of 675±15 m/sec. Recording of the dependence of specimen free surface velocity on time is similar of the dependence given in [11] for the same test arrangement. Metallographic analysis of the preserved central section of a specimen with a diameter of about 40 mm showed the following. In an etched microsection macroscopic spalling was not observed visually in the specimen. With study of the microsection under a microscope in the central zone where the variable-capacitance transducer was located spalling microdamage was noted, which may be classified as intense. Several merging microcracks, forming as it were a main microcrack, are located at a distance of 0.75 mm from the free surface. Separated individual microcracks are visible at distances of 0.4, 0.5, and 1.0 mm from the free surface.

Microspecimens were prepared for determining material residual mechanical properties from a reference specimen and from several shock-loaded specimens. Microspecimens were cut from the central zones of macrospecimens coaxially with the shock-wave loading direction. They had a diameter of 1 mm and a gage length of 5 mm. The tensile diagrams obtained for microspecimens cut from macrospecimens shock-loaded at normal temperature are given in Fig. 2. Marked with an asterisk is the average tensile diagram for six tests on a reference specimen, and almost coinciding with it is the average diagram for seven tests on a specimen shock-loaded at a rate of 80 m/sec, and also diagrams for microspecimens cut from a macrospecimen shock-loaded at a rate of 105 m/sec.

Average values for the rest of the mechanical properties of macrospecimens in the longitudinal direction with respect to the loading direction are given in Table 1. The mean square deviation is indicated here as a scatter characteristic.

The original structure of the test alloy is characterized by a considerable number of inclusions whose location coincides predominantly with the plane of the sheet. The average microhardness determined on the basis of fifteen measurements is (615±25) MPa. The nature of the following stages of alloy spalling failure at normal temperature is given in Fig. 3. Small ductile microcracks and pores form as a rule at inclusions (a). Then there is merging of damage located in a single plane (b) and in parallel planes with formation of larger ductile cracks. The nature of spalling failure for a specimen shock-loaded by a foil according to the procedure in [11] is similar to the nature of microfailure given in (b). The nature of subsequent stages of spalling failure for the alloy at 500°C is indicated in Fig. 4. In this case there is a reduction in the overall concentration of spalling microdamage (a), it is more ductile in nature (b), and interaction and merging is connected with considerable local shear strain for the material.

An initial attempt at determining the temperature dependence of spalling resistance for the alloy was made in [9]. However, here the degree of spalling failure was only determined visually from swelling either with separation of the rear surface from the specimen or with observation of a polished cross section. In view of this the results obtained only characterize the condition for development of macroscopic spalling failure of the alloy. Subse-

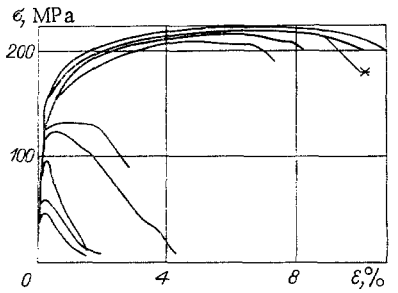


Fig. 2

quently [10], more detailed metallographic analysis was carried out for test specimens, and a number of additional tests were also completed with the aim of determining conditions corresponding to the initial stage of spalling failure for the alloy at normal test temperature. In this work conditions were also clarified for spalling failure initiation at 500°C in bar specimens tested previously. However, the main work was preparation of new experimental results for the effect of temperature on the spalling failure of alloy AMg6 specimens prepared from sheet and subjected to annealing. For these specimens with two test temperatures, i.e., normal and 500°C, the range of shock-wave loading from spalling microdamage initiation to complete macroscopic spalling failure was determined quite accurately.

Joint consideration of all of the experimental results for the effect of temperature on spalling failure for alloy AMg6 given in Fig. 1 makes it possible to draw the following suggested conclusions. Alloy specimens tested in the two cases considered in Fig. 1 differ in two main technological factors. First, a preferred direction of fiber structure. For bar specimens it is coaxial with the loading direction, and for sheet specimens it is perpendicular. Second, the initial specimen material condition. As test hardness measurements have shown bar material is initially in the cold-worked condition, and sheet is annealed. Additional annealing of the prepared specimens served here in a certain sense as an insurance measure for clear conclusiveness of the data obtained for spalling resistance. Thus, the considerable excess of bar specimen resistance compared with sheet is due to the effect of both of these factors. To what extent for each of these. Evidently it is possible to suggest the following.

The original condition of the alloy affects to a considerable degree the conditions for initiation of spalling microdamage at normal temperature, i.e., whether it is in the cold-worked, previously deformed condition, or it was annealed in order to remove internal stresses and distribute intermetallic inclusions more uniformly. To some degree this is confirmed by the fact that with heating to 500°C when bar material would undergo rapid annealing, critical conditions for spalling microdamage initiation become the same for both materials. In this connection it is also possible to mention results in [14] in which a study was made of aluminum alloy 6061 in the thermally hardened condition. It was shown that the direction of the fibrous structure caused by directional rolling of blanks does not affect the critical stress corresponding to spalling microdamage initiation. At the same time, prior annealing led to a marked reduction by more than 30% of the spalling resistance for the alloy determined in this way. It was also noted in [15] for alloy 6061 that in specimens prepared from bar and sheet, initiation of spalling damage occurs under the same loading conditions. However, it is not possible to ignore the existence of a contrasting example from [16] where a study was made of aluminum alloy 2024. Here with the same loading conditions for specimens cut from bar coaxially and perpendicular to the rolling direction, in the first no spalling microdamage is determined, whereas in the second there is intense microfailure.

Concerning conditions of complete macroscopic spalling failure for the alloy at normal temperature, then here apart from the original condition the primary direction of the fibrous structure has an important effect, i.e., ths drawn out nature of grains and chains of inclusions in the rolling direction. In the initial stage of spalling failure processes of initiation, development, and merging of spalling damage in the form of ductile microcracks occurs predominantly in the direction of the fibrous structure. Therefore, the process of spalling failure for bar specimens is considerably more energy consuming since it includes, as it were, an initial stage of merging by breaking of bridges for damage zones drawn out in the longitudinal direction. This also explains the considerably higher critical loading

TABLE 1

| Test conditions | $\sigma_{0,2}$, MPa | $\sigma_f$, MPa | $\delta$, % |
|---|---|---|---|
| Control sample | 158±10,6 | 217±4,5 | 9,8±1,1 |
| $T \simeq 0$, $w = 80$ m/sec | 159±8,4 | 219±3,7 | 9,7±0,9 |
| $T \simeq 0$, $w = 105$ m/sec | 112±41 | 137±69 | 4,7±3,4 |
| $T = 500$°C, $w = 77$ m/sec | 145±6,3 | 212±2,4 | 11,9±0,6 |
| $T = 500$°C, $w = 103$ m/sec | 101±55 | 105±58 | 4,6±2,7 |

level for bar material corresponding to complete macroscopic spalling failure at normal temperature. An increase in temperature to 500°C leads to the fact that failure becomes more ductile and less dependent upon the direction of the fibrous structure. Therefore, critical spalling macrofailure and microfailure conditions for both types of material become similar, and in fact identical.

Separate and no less important is the question of the effect of loading time on the spalling resistance of alloy AMg6, as for other structural materials. Such data were obtained in [7, 8] for bar and sheet materials by changing the scale of the striker–specimen system during loading. Careful consideration of these results, and also the fact known from the literature cited that bar alloy AMg6 is normally supplied in the cold-worked condition and sheet in the annealed condition, makes it possible to compare the results of these works with those obtained by us. For this purpose we briefly mention the methodology for revealing the degree of spalling damage for specimens in [7, 8]. Recording of spalling damage was carried out in these works visually at low optical magnification. This method makes it possible with a sufficiently well polished microsection to reveal as the initial stage of spalling damage the stage of intense microscopic failure. Two critical loading conditions were considered leading to development of local damage in the form of pores or isolated cracks and joining of local damage into a spalling crack. In the light of our data obtained with the use of detailed metallographic analysis of test specimen microsections, the values given in [8] relating to the critical loading levels mentioned may be treated thus. At the lower limit, corresponding to the development of local damage, the degree of spalling damage for the material is weak and net revealed visually with a small increase in microfailure. At the upper limit, corresponding to merging of local damage into a spalling crack, the degree of spalling damage may be treated as partial spalling failure for the specimen material. From the known impact velocity we make the same estimates adopted by us for pressure in the loading pulses and typical loading time. Comparison of the results obtained for the effect of typical loading time on spalling failure of bar (a) and sheet (b) specimens of alloy AMg6 is given in Fig. 5 (labeling the same as in Fig. 1), and the conditions for weak microfailiure are indicated by a broken-dotted line. The good conformity obtained previously [7, 8, 10] and in this work for results of alloy failure at normal temperature, and the joint consideration of them, has made it possible to clarify the time dependence for critical loading level corresponding to initiation of spalling microdamage.

There is quite good agreement of the data in question and results obtained with specimen loading by the procedure in [11]. Here specimen loading emerging at the free surface with a pressure pulse of 2.05 GPa and loading determined typically at the half-height of time 0.25 μsec led to intense microfailure to a depth of 0.75 mm. The result obtained for the degree of spalling damage completely agrees with those given in Fig. 5 for annealed sheet material. As far as the results obtained by the method in [11] for recording stress relaxation and the conclusion based on them about the spalling resistance of alloy AMg6 with short loading times are concerned, then here it is possible that a specific role is played by individual areas of microdamage to a depth of 0.4 and 0.5 mm, located by the way in the direction of the main microcrack, which could distort the picture for recording the actual failure process occurring with higher tensile loads. The final answer to this question could be given by a similar test with a pressure pulse less than 1.65 GPa emerging at the free surface, i.e., with loading parameters not leading to a spalling failure process revealed microscopically. Data in [12, 13] are in agreement with the results obtained.

The question also remains of the quantitative extent of spalling damage for the material. In the nominal qualitative grading of the degree of spalling failure adopted by us for specimens, only the first and final stages are absolutely determined, i.e., when in the specimen cross section spalling microdamage is generally not observed, and when a macroscopic spalling

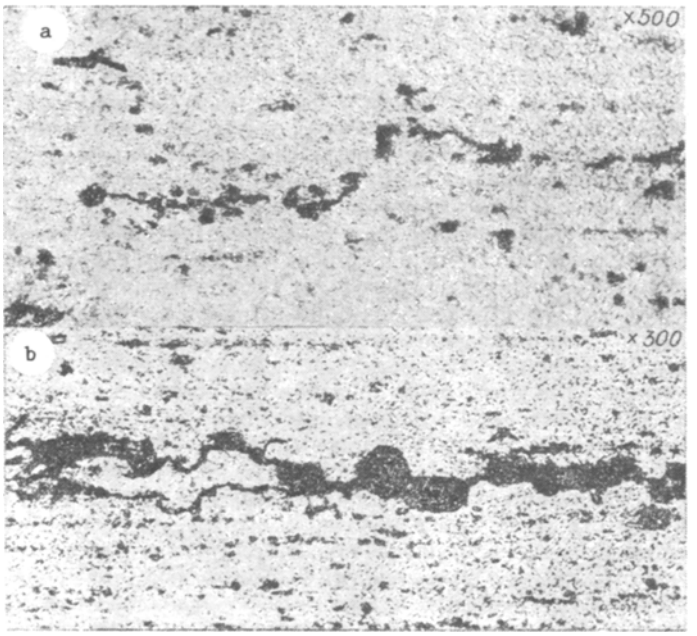


Fig. 3

crack passes through the whole of its cross section. A quantitative method for determining material spalling microdamage is for example the method of detailed computation of the amount and size of spalling damage formed and determination finally of its total specific volume, and also a method for determining the residual static strength of specimens cut from shock-loaded spalling-damaged targets. The first of the methods was used in [17] in revealing the degree of spalling damage for aluminum, and the second in [18] for determining the residual strength of spalling-damaged specimens of aluminum alloy type V95. In the latter work quite large specimens were tested, which made it possible to obtain adequately averaged residual strength values. In this work determination of residual properties of some shock-loaded specimen targets was carried out in microspecimens.

With regard to the specific results obtained in this work, it is possible to note the following. After loading at normal temperature residual mechanical properties for the first of the specimens in which no spalling microdamage was detected remained at the level of the properties of the reference specimen with a very weak tendency towards strengthening and a more clearly defined tendency towards levelling caused by a reduction in the scatter of all of the mechanical properties. For the second of the specimens for which the degree of spalling damage was estimated qualitatively as work microfailure, the values of average strength and elongation realized were 63 and 48% of the original values. After loading at 500°C the residual properties of the first of the specimens for which spalling microdamage was not detected a small reduction in strength and increase in ductility is typical, which is mainly due to the effect of annealing. To an even greater degree a tendency is observed towards the levelling of mechanical properties. By assuming that the properties of this specimen are the originals, we estimate the reduction in mechanical properties of the second of the specimens whose degree of spalling damage was estimated qualitatively as intense microfailure. Values of average and relative elongation realized in this case were 49 and 38% of the original values. Thus, a quite good correlation exists between qualitative and quantitative estimates of the degree of spalling damage.

With regard to the possibility of comparing values of alloy ultimate strength with uniaxial dynamic tension and spalling resistance characterizing the conditions for spalling damage initiation, it is possible to note the following. The mechanical properties of alloy AMg6, in particular ultimate strength, according to data in [1-5] depend quite weakly on deformation rate up to a value of $10^4$ $sec^{-1}$. By neutralizing certain contradictions of other works it is even possible to assume conditionally that it is not sensitive to deformation rate in the range in question. Starting from a deformation rate of $10^4$ $sec^{-1}$ or more, the tendency towards an increase in its strength is overlooked [6], and therefore in the intermediate range of typical loading times $10^{-5}$-$10^{-6}$ sec data for dynamic strength under uniaxial

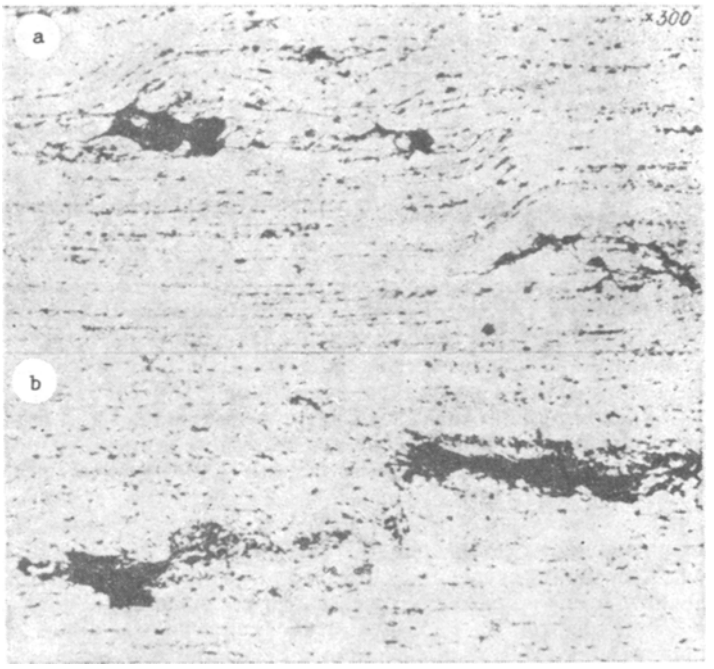


Fig. 4

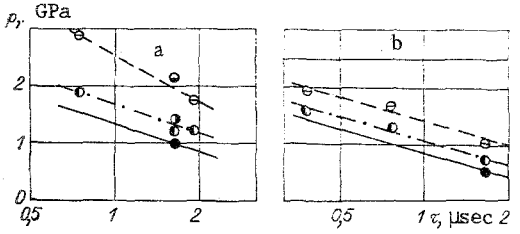


Fig. 5

tensile conditions and for spalling resistance may be joined conditionally by a smooth interpolation dependence of strength on loading time.

Thus, combined analysis of existing experimental data for spalling damage of aluminum alloy AMg6 with shock-wave loading has shown that they agree quite satisfactorily with each other if in considering temperature and time dependences for spalling resistance notice is taken of questions of preparation technology and prior material treatment. To an equal extent this undoubtedly also relates to all other structural materials.

## LITERATURE CITED

1. V. P. Krashchenko, N. P. Rudnitskii, et al., "Mechanical properties of AMg6M alloy over wide ranges of temperature and deformation rate," Probl. Prochn., No. 6 (1985).
2. P. G. Miklyaev and V. M. Dudenkov, Resistance to Deformation and Ductility of Aluminum Alloys (Handbook) [in Russian], Metallurgiya, Moscow (1979).
3. N. N. Beklemeshev, V. V. Gribkov, et al., "Study of the mechanical properties of aluminum alloys D16 and AMg6 with dynamic loading using annular specimens," in: Plastic Deformation of Light and Special Alloys [in Russian], Metallurgiya, Moscow (1978).
4. A. P. Bol'shakov, S. A. Govikov, and V. A. Sinitsyn, "Study of dynamic diagrams for uniaxial tension and compression of copper and alloy AMg6," Probl. Prochn., No. 10 (1979).

5. N. N. Popov, A. G. Ivanov, et al., "Preparation of complete uniaxial tensile diagrams for alloys AMg6 and MA18 with deformation rates of $10^{-3}$-$10^{3}$ $sec^{-1}$," Probl. Prochn., No. 12 (1981).
6. G. V. Stepanov, V. V. Astanin, et al., "Mechanical properties of high-strength aluminum alloy with shock loading," Probl. Prochn., No. 2 (1983).
7. B. A. Tarasov, "Quantitative description of spalling damage," Zh. Prikl. Mekh. Tekh. Fiz., No. 6 (1973).
8. B. A. Tarasov, "Resistance to failure of plates with shock loading," Probl. Prochn., No. 3 (1974).
9. E. V. Bat'kov, S. A. Novikov, et al., "Effect of specimen temperature on the value of failure stresses with spalling in aluminum alloy AMg6," Zh. Prikl. Mekh. Tekh. Fiz., No. 3 (1979).
10. V. K. Golubev, S. A. Novikov, et al., "Nature of spalling failure for aluminum and its alloys D16 and AMg6 in the temperature range −196 to 600°C," Probl. Prochn., No. 2 (1983).
11. G. I. Kanel', S. V. Razorenov, and V. E. Fortov, "Failure kinetics for aluminum alloy AMg6M under spalling conditions," Zh. Prikl. Mekh. Tekh. Fiz., No. 5 (1984).
12. B. I. Abashkin, I. Kh. Zabirov, et al., "A method for studying material properties with dynamic tension," Zh. Prikl. Mekh. Tekh. Fiz., No. 4 (1977).
13. V. K. Golubev, S. A. Novikov, et al., "Effect of shock-wave emergence angle at the free surface on formation of spalling in metals," Zh. Prikl. Mekh. Tekh. Fiz., No. 3 (1983).
14. B. W. Butcher, "Spallation in 6061-T6 aluminum," in: Behavior of Dense Media Under High Dynamic Pressures, Gordon and Breach, N.Y. (1968).
15. D. W. Blincow and D. Y. Keller, "Experiments on the mechanism of spall," in: Dynamic Behavior of Materials, ASTM, Philadelphia (1963).
16. Z. Rosenberg, G. Luttwak, et al., "Spall studies in differently treated 2024 Al specimens," J. Appl. Phys., 54, No. 5 (1983).
17. T. W. Barbee, L. Seaman, et al., "Dynamic fracture criteria for ductile and brittle metals," J. Mater., 7, No. 3 (1972).
18. V. I. Romanchenko, O. I. Marusii, and I. V. Kramarenko, "Microstructure of aluminum alloy in the early stages of spalling," Probl. Prochn., No. 9 (1983).